An Case Study on the Lomer-Cottrell Junction in FCC Metals

July 23, 2007

Seokwoo Lee and Wei Cai
(*Stanford University*

This report is based on two papers: "*From Dislocation Junctions to Forest Hardening*, Phys. Rev. Lett. **89** 255508 (2002), R. Madec, B. Devincre, and L. P. Kubin "and "*Structure and Strength of Dislocation Junctions: An Atomic Level Analysis*, Phys. Rev. Lett. **82** 1704 (1999), D. Rodney and R Phillips ".

1 Introduction

Heisenberg's uncertainty principle tells us the fundamental limitation of observation in small scale; if the size of a object is very small, there should be an uncertainty of measurements of its exact position and momentum simultaneously. Although the physical characteristic is different, in the case of the mechanical properties of metals in small scale, "Smaller is more uncertain" phenomena happen when we try to measure mechanical properties of metals.

Plastic deformation of metals is usually governed by the motion of dislocations and their reactions, such as nucleation, pinning, and multiplication. In general, since the number of dislocations is very high in large scale, the plastic deformation behavior arises from the average response of a whole dislocation structure under a given stress. If a sample is produced in the same way and stresses are applied in the same crystallographic direction, we can obtain fairly the consistent properties even though the detailed initial configurations of dislocations are different. However, this is not true in small scale. As a sample gets smaller, the number of dislocation becomes lower. From a certain size, the distribution of dislocation begins to be not uniform any more, and the average effect breaks down. Thus, the mechanical properties in small scale depend strongly on the initial configurations of dislocations. However, the problem is that there is no experimental technique to describe those configurations precisely. The transmission electron microscope (TEM), the conventional way to observe dislocations, requires the sample thickness less than 1000 Å for the transmission

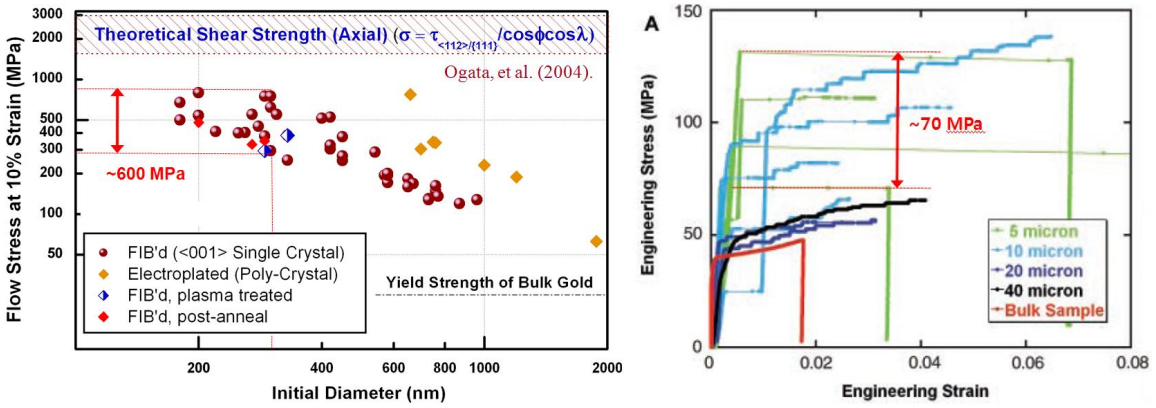

Figure 1: The variation of yield strengths (Reproduced by Prof. Nix's kind permission)

of electrons. Thus, it is impossible even to see dislocations in a sample with a thickness larger than 1000 Å. Even though the size is smaller than 1000 Å, the acquired images from TEM are just the projected ones. In sum, there is a limitation to observe the initial configuration of dislocations before deformation.

The limitation of observation gives the uncertainty of mechanical properties in small scale. In conventional experiments, the sampled configurations of dislocations are usually very different even though the samples are produced in the same way. Since it is impossible to figure out those configurations precisely, we cannot obtain the determistic mechanical properties. This uncertainty is much larger in small scale because the initial configuration dependence of mechanical properties is higher in small scale, as already mentioned. Thus, we cannot help measuring the different mechanical properties in small scale for each same experiment. For example, in Greer's and Uchic's results, it is found that they got large variations of yield strengths in Fig. 1 in spite of the same sized samples [?, ?].

In sum, in small scale, uncertainty of measurements seems to be unavoidable in experiments. However, this is not pessimistic since we can make this uncertainty more determistic by the comparative study between experiments and simulations. The formation and dissociation of the Lomer-Cottrell junction governs the hardening of fcc crystals. In small scale, the number of junction becomes small, and each junction plays more important role in hardening behavior. Thus, this DDLAB case study of the individual Lomer-Cottrell junction in fcc crystals (Gold) can be more meaningful in small scale. In this report, the initial configuration dependence on the junction lengths and the corresponding critical stresses needed to dissociate the junction are studied.

2 DDLAB coding

Only the main parts of the codes are provided in this section to save the space. The whole codes are attached in **Appendix**.

2.1 The initial configuration of two dislocations

Following the initial configurations of two dislocation in Madec's paper, it is needed to generate two dislocation sets with the same length on $(1\,1\,1)$ and $(1\,1\,\bar{1})$ planes. The Lomer-Cottrell junction forms on the intersection of these two planes along $[\bar{1}\,1\,0]$ direction. Mathematically, we can make a circle by a parametric representation form. If the θ is the parameter and the point $\mathbf{P}$ on the circle is given by

$$\mathbf{P} = R\cos(\theta)\mathbf{u} + R\sin(\theta)\mathbf{n} \times \mathbf{u} + \mathbf{c},$$

where $\mathbf{u}$ is a unit vector from the center of the circle to any point on the circumference; R is the radius; $\mathbf{n}$ is a unit vector perpendicular to the plane and $\mathbf{c}$ is the center of the circle. Here, for two dislocation sets, the normal vectors, $\mathbf{n}$, are $[1\,1\,1]$ and $[1\,1\,\bar{1}]$ and the $\mathbf{c}$ is the origin. θ is defined the angle between the dislocation lines and the instersection, so $\mathbf{u}$ is taken as $[1\,\bar{1}\,0]$. Using this form, we can construct the circle as described by Fig. 2. The corresponding MATLAB code is represented as below.

```
% Make dislocations
t = [-1:0.1:1]*pi;

x = 2000*(-cos(t)/sqrt(2)-sin(t)/sqrt(6));
y = 2000*(cos(t)/sqrt(2)-sin(t)/sqrt(6));
z = 2000*(2*sin(t)/sqrt(6));

x1 = 2000*(-cos(t)/sqrt(2)+sin(t)/sqrt(6));
y1 = 2000*(cos(t)/sqrt(2)+sin(t)/sqrt(6));
z1 = 2000*(2*sin(t)/sqrt(6));

figure(2)
plot3(x,y,z,'-o', x1,y1,z1,'-o');
xlim([-2500 2500]);ylim([-2500 2500]);zlim([-2500 2500]);
grid on
view([30 -30 40])
```

Each circle has 20 points. If we define a dislocation line by connecting one point and its origin-symmetric point, we can obtain 20 dislocations for each circle.

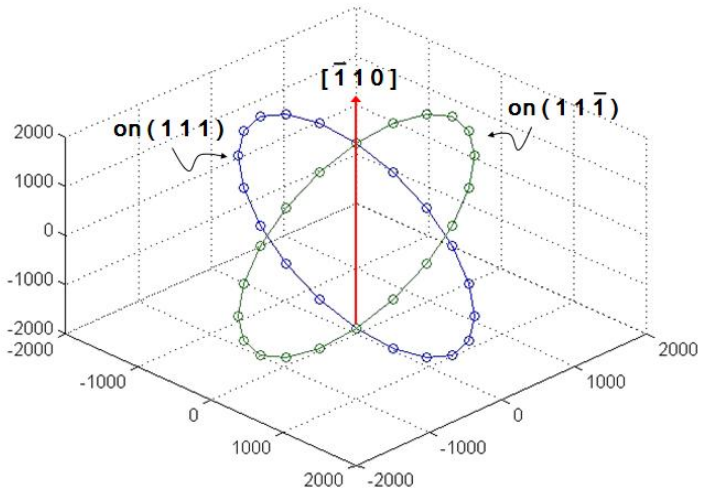

Figure 2: The start and end points of each dislocation lines on on (1 1 1) and (1 1 $\bar{1}$) planes. (The whole MATLAB code is in **Appendix**.)

2.2 Mobility law of an FCC crystal

In DDLAB, the motion of dislocations is expressed by the motion of nodes. Thus, the computation of nodal velocities is important part of dislocation dynamics simulation. How dislocation move is largely controlled by the atomistic structures and energetics of dislocation core, which can vary significantly from one dislocation (or material) to another. Thus, the dislocation mobility is strongly materials specific. For example, in bcc crystals, dislocation do not dissociate into partials. However, the core of screw dislocation in fcc crystals splits planarly into two partials on (1 1 1) planes, bounding a stacking fault area, as shown in Fig. 3(a). Since the stacking fault energy is low on { 1 1 1 } planes, the dislocation core prefers to spread itself on one of those planes. Thus, the motion of bounded partial dislocations is entirely confined within the initial dissociation plane. In real FCC crystals, cross slip also happen during deformation, as shown in Fig. 3(b). For example, for a dislocation with Burgers vector $1/2[\,1\,\bar{1}\,0\,]$, its glide plane could be either (1 1 1) or (1 1 $\bar{1}$). However, cross slip is more energetically unfavorable than the glide motion, the cross slip probability is ignored in DDLAB.

For simplicity, dislocation velocity is assumed to be isotropic within the glide plane and to be linear to the driving force (because the Peierls stress in FCC metals is very low). Thus, we can express a mobility law in FCC crystals by a single parameter M,

$$\mathbf{v} = M \cdot \mathbf{f} - M \cdot (\mathbf{f} \cdot \mathbf{n}) \cdot \mathbf{n}$$

The second term ensures that velocity $\mathbf{v}$ remain orthogonal to glide plane normal $\mathbf{n}$.

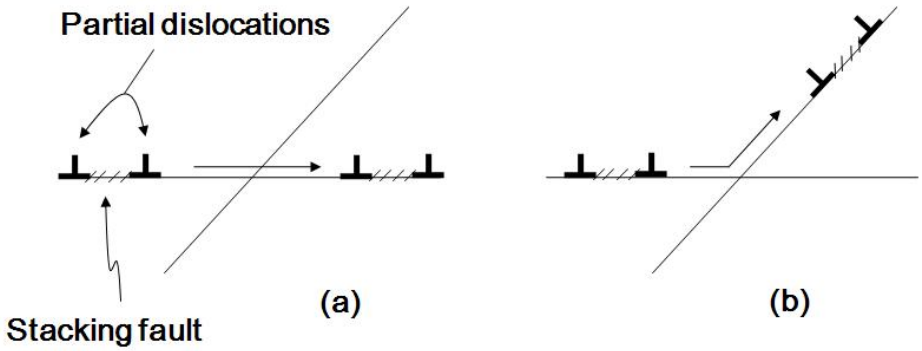

Figure 3: (a) The glide motion and (b) cross slip of two partial dislocations in fcc metals.

2.3 The calculation of junction lengths

With the obtained dislocation sets in section 2.1 we can find each junction length for 400 (20×20) binary dislocations. Since we wanted to see junction formation without an external stress, the applied stress was set as zero. For each dislocation set, the normal vectors of slip plane were set as $[\,1\,1\,1\,]$ and $[\,1\,1\,\bar{1}\,]$ in Madec's way, and Burgers vectors were chosen as $1/2[\,1\,0\,\bar{1}\,]$ and $1/2[\,0\,1\,1\,]$, respectively. Shear modulus is chosen as that of gold (27 GPa). As mobility function, `mobfcc1.m` was used for fcc crystals. These values are fixed, then simulations were performed only by changing dislocation line directions. In order to compute effectively, 'for-loop 'was used.

```
totalsteps=100;
appliedstress = zeros(3,3);
mobility='mobfcc1';

make_dis;

for dis1_no=1:21;
    for dis2_no=1:21;

rn = [  D1(dis1_no,:)                  7
        0      0      0     0
       -D1(dis1_no,:)                  7
        D2(dis2_no,:)                  7
        0      0      0     0
       -D2(dis2_no,:)                  7 ];

b1 = [  1   0  -1  ]/2;
b2 = [  0   1   1  ]/2;
```

```
n1 = [  1   1   1  ];  % no glide constraint
n2 = [  1   1  -1  ];  % no glide constraint

links = [ 1 2   b1 n1
          2 3   b1 n1
          4 5   b2 n2
          5 6   b2 n2 ];

.....................................
(other inputs: See Appendix.)
.....................................

dd3d;

move_pos = find(rn(:,4)==0);
move_coord = [rn(move_pos,1) rn(move_pos,2), rn(move_pos,3)];
junc_pos = find(-10^-2<move_coord(:,3) & move_coord(:,3)<10^-2 );

    if length(junc_pos)==1;
        junc_length(dis1_no,dis2_no)=0;

    elseif isempty(junc_pos)==0;
        junc_coord = [move_coord(junc_pos,1) move_coord(junc_pos,2),...
         move_coord(junc_pos,3)];
        junc_max = find(max(junc_coord(:,1)));
        junc_length(dis1_no,dis2_no) = sqrt(2)*...
        sqrt(junc_coord(junc_max,1)^2+junc_coord(junc_max,3)^2...
        +junc_coord(junc_max,3)^2);

    elseif isempty(junc_pos)==1;
        junc_length(dis1_no,dis2_no)=0;

    end
    end
end
```

2.4 The critical stresses required to break the junctions

Based on Rodney's paper, the shear stress was applied on $(1\,1\,1)$ plane, as described in Fig. 4. The coordinate system is already set up as $\mathbf{e_1} = [1\,0\,0]$, $\mathbf{e_2} = [0\,1\,0]$, and $\mathbf{e_3} = [0\,0\,1]$. Thus, in order to apply the shear stress on $(1\,1\,1)$ plane, stress transformation is needed. As described in Fig. 4, the new coordinate system was chosen as $\mathbf{e'_1} = [\bar{1}\,\bar{1}\,2]$, $\mathbf{e'_2} = [\bar{1}\,1\,0]$, and $\mathbf{e'_3} = [\bar{2}\,\bar{2}\,\bar{2}]$.

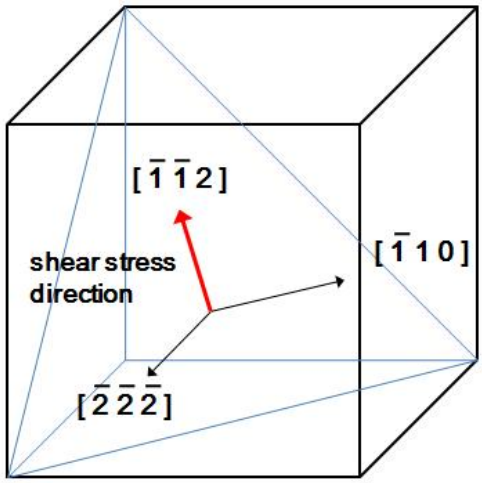

Figure 4: The new coordinate system for the stress transformation.

The stress transformation can be performed by the relation,

$$\boldsymbol{\sigma'} = \mathbf{A}\boldsymbol{\sigma}\mathbf{A}^{\mathbf{T}},$$

where $\boldsymbol{\sigma'}$ and $\boldsymbol{\sigma}$ are the stress tensors defined in the new and old coordinate system, respectively (The axes of the old coordinate are $\mathbf{e_1}$ =[1 0 0], $\mathbf{e_2}$ =[0 1 0], and $\mathbf{e_3}$ =[0 0 1]). $\mathbf{A}$ is the transformation matrix which components are consisted of directional cosines. Since the applied stress in DDLAB are set up in the old coordinate system, we have to transform the known stresses in the new coordinate system. Therefore, we need the transformation of

$$\boldsymbol{\sigma} = \mathbf{A}^{-1}\boldsymbol{\sigma'}\mathbf{A}^{\mathbf{T}-1}.$$

The applied stresses are increased manually (like the experiment!). The MATLAB code is represented as below.

```
load junction_data_1

totalsteps=600;

%stress in coordinate system 1
sigma = [ 0    0  0.6
          0    0  0
          0.6  0  0 ] * 1e8;   %in Pa
%coordinate system 1
e1 =  [-1 -1 2]; e2  = [-1 1 0]; e3 = [-2 -2 -2];
e1=e1/norm(e1); e2=e2/norm(e2); e3=e3/norm(e3);
%coordinate system 2 (cubic coordinate system)
```

```
e1p = [1 0 0]; e2p = [0 1 0]; e3p = [0 0 1];
e1p=e1p/norm(e1p); e2p=e2p/norm(e2p); e3p=e3p/norm(e3p);
%rotation matrix
T = [ dot(e1,e1p) dot(e1,e2p) dot(e1,e3p)
      dot(e2,e1p) dot(e2,e2p) dot(e2,e3p)
      dot(e3,e1p) dot(e3,e2p) dot(e3,e3p) ];

%Transform stress into current coordinate system
appliedstress = T^-1*sigma*(T^-1)';
```

3 Results and Discussion

3.1 The initial configuration dependence on the junction lengths

During the relaxation, the Lomer-Cottrell junction was formed as described in Fig. 5. As expected, it forms along the $(\bar{1}10)$ direction on the intersection of two slip planes.

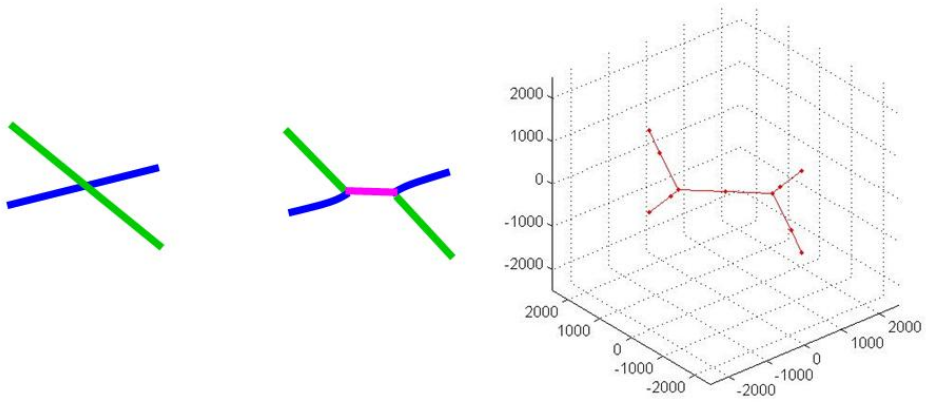

Figure 5: The Lomer-Cottrell junction formation

The junction lengths could be calculated from `rn` matrix, which includes the coordinate number of each node by the following step.

1. Exclude the coordinate numbers including the end point, which have 7 in the forth column.
2. Find the coordinate numbers with zero in the third column.
3. Then, find the vector with the maximum component in the first or second column.
4. (Junction length) = $\sqrt{2}\times$(the obtained maximum component)

```
rn = 1.0e+003 *
    0.6642   -1.6240    0.9598    0.0070
    0.6738   -0.6738   -0.0000         0 <--
   -0.6642    1.6240   -0.9598    0.0070
    0.6642   -1.6240   -0.9598    0.0070
   -0.6642    1.6240    0.9598    0.0070
    0.6484   -0.9419    0.2935         0
   -0.6484    0.9420   -0.2936         0
    0.0070   -0.0065    0.0000         0
   -0.6739    0.6739    0.0000         0 <--
```

```
 0.6765   -1.2658   -0.5893         0
-0.6764    1.2678    0.5914         0
```

Thus, in the case of this example, the junction length can be calculated approximately by

(Junction length) = $\sqrt{2}\times 673.9 = 952.6143$.

Notice that using this method, we cannot find the junction length in the extreme cases; for example, $\phi_1 = 0$, $\phi_2 = 0$. However, intuitively, the junction length is the same with the initial dislocation length in this case. Thus, the obtained matrix of the junction length was modified as below.

```
% Modification of junction lengths at the extreme angles
junc_length(1,1)=2000;
junc_length(21,1)=2000;
junc_length(1,21)=2000;
junc_length(21,21)=2000;
junc_length(11,11)=2000;
```

Furthermore, for some dislocation sets, the calculated junction lengths are not correct because *merge* effect. In fact the node at the end of junction has to connect junction to two dislocation arm. However, during the formation of junction, if the node at the end of junction become too close to the fixed node at the end of dislocation arm, two nodes merge together. Thus, it looks like one junction and one arm structure (not two arms!). Thus, since the above code cannot consider this case, we have to correct the obtained `junc_length` matrix manually. Here, the merge effect occurs at 7 sets; `(D1, D2) = (21,1), (1,20), (3,20), (20,21), (21, 20), (10,11), (11,10)` (It is not difficult to find these sets because there should be lower junction lengths than you expected at the first obtained plot). The junction length of these sets is 2000. Finally, we can obtain the initial configuration dependence on the junction lengths for every dislocation couple as described in Fig. 6. The Medec's result is also included.

3.2 The critical stresses needed to break junctions

When a shear stress larger than a critical stress was applied, the Lomer-Cottrell junction was dissociated as described in Fig.8.

The critical stresses needed to dissociate the junction was obtained by the manually increase of `simga`. The stability of junctions depends on the length of dislocation arm (l) as depicted in Fig. 8. Since the two end nodes of dislocation arm are fixed,

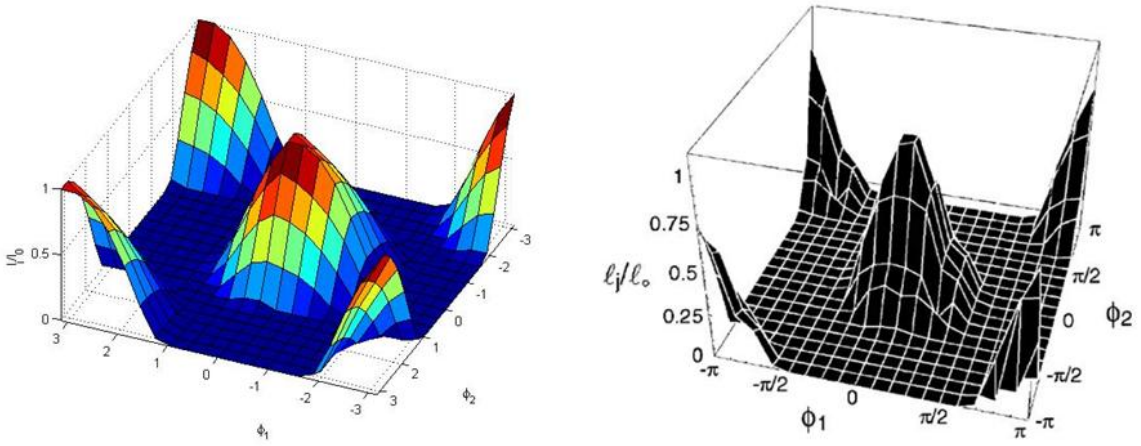

Figure 6: The initial configuration dependence on the junction lengths. The left one is the result of this study, and the right one is Medec's result.

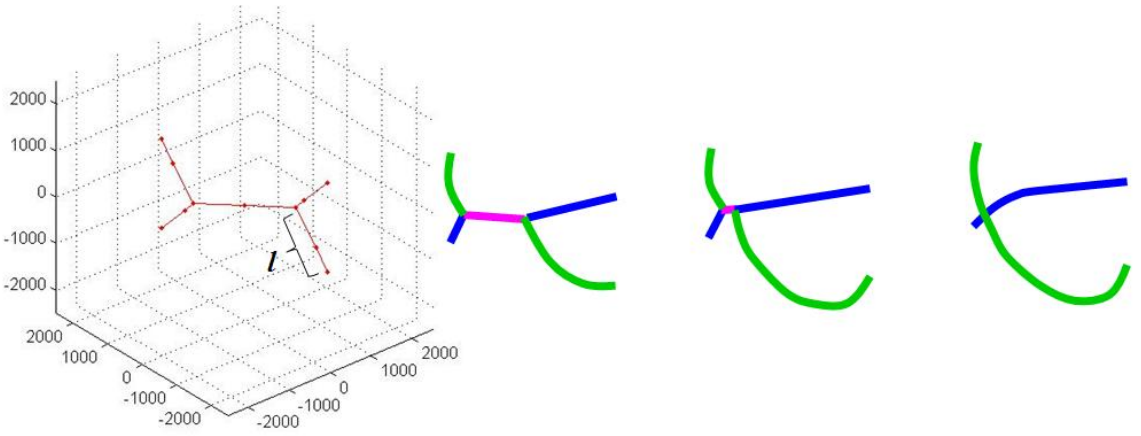

Figure 7: The dissociation of Lomer-Cottrell junction

it behaves as the Frank-Read source. The junction can be broken when one of dislocation arms bows out under a stress larger than a critical stress. The critical stress needed to bow out can be obtained roughly by the relation

$$\sigma_c \approx \frac{\mu b}{l},$$

where μ is the shear modulus, b the size of Burgers vector and l the length of dislocation arm. The dissociation can occur more easily as the dislocation arms are long because the critical stress is low by the above relation. If the initial length of two dislocations increases, the lengths of junctions get longer. Also, the length of dislocation arms become longer (not shown), resulting in the low critical stresses needed for dislocation arms to bow out.

Firstly, let's change the configuration (the dislocation line direction) without changing the initial length of dislocations. Since the initial length of dislocations are same,

when the junction length is longer, the length of dislocation arm is shorter. Thus, in this case, it is easier to dissociate the junction with the longer length. The obtained values are tabulated in the table below. Then, this result is plotted in Fig. **??**.

ϕ_1 (rad)	ϕ_2 (rad)	junction length (nm)	τ_c (MPa)
$3\pi/10$	$1\pi/10$	466	20
$3\pi/10$	$2\pi/10$	397	16
$3\pi/10$	$3\pi/10$	259	14
$3\pi/10$	$4\pi/10$	102	13

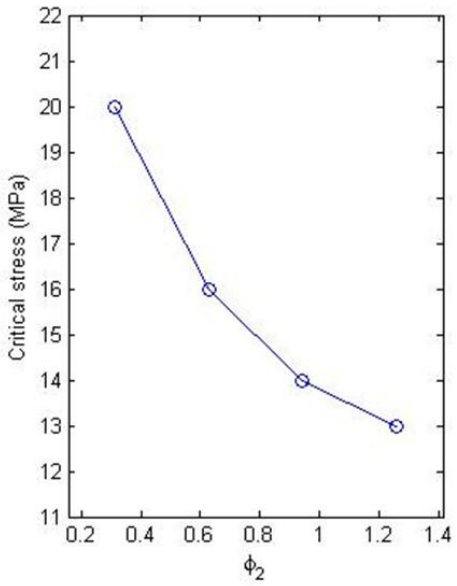

Figure 8: The initial configuration dependence on the critical shear stress required for the dissociation of junction.

As mentioned early, if the externals size of a sample is smaller, the yield strength gets higher. This is so-called "Smaller is Stronger "phenomenon. Recently, there are many models to explain this phenomenon; for example, Nix's dislocation starvation model, Uchic's source deactivation model, and Tang's dislocation escape model. In this study, we can find one more view. Usually, a sample is made from the thin film deposition. During that time, dislocations forms, then, followed by annealing. If the deposited film is thin ($1\sim2\ \mu m$), the length of dislocations distributed in the sample before annealing must be short. It means that after annealing, junctions have the shorter dislocation arms than those in bulk metals. Thus, we need the larger stress to dissociate the junctions. This could be one contribution of "Smaller is Stronger "phenomenon. The initial dislocation length dependence on junction length and critical stress required for the dissociation of junction are plotted in Fig. 9. Here, both ϕ_1 and ϕ_2 are selected as $\pi/10$.

As shown in Fig. 10, as the initial dislocation length is smaller, the larger shear stress is needed to dissociate junction.

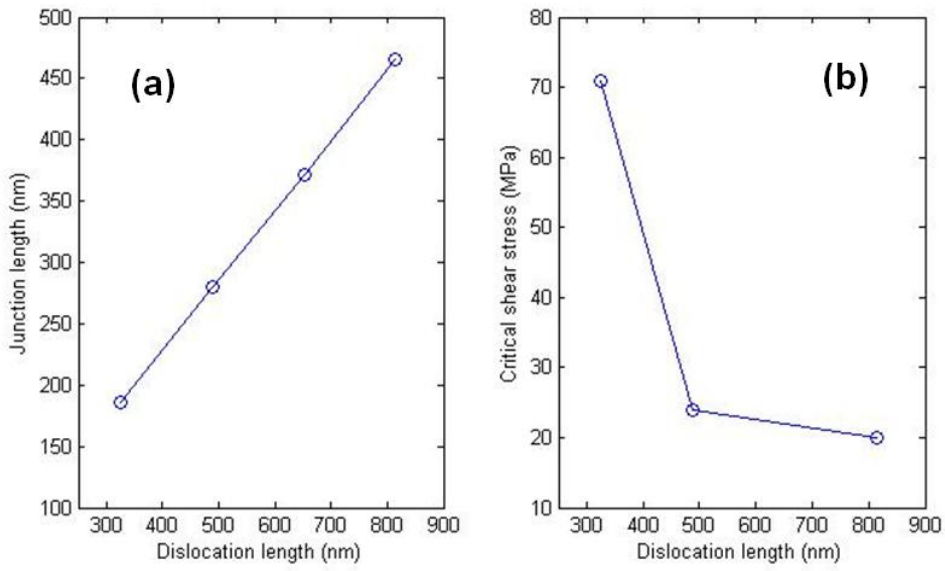

Figure 9: Junction length dependence on the critical shear stress on (1 1 1) plane and junction direction dependence on the critical stress.

4 Conclusion

The formation and dissociation of the Lomer-Cottrell junction governs the hardening of fcc crystals. In small scale, the number of junction becomes small, and each junction plays more important role in hardening behavior. Thus, this DDLAB example study of the individual Lomer-Cottrell junction in fcc crystals can be more meaningful in small scale. In this report, the initial configuration dependence on the junction lengths and the corresponding critical stresses needed to dissociate the junction are studied. The junction length are largely dependent of the initial configuration of dislocations. A critical stress need to dissociate the junction depends on the initial dislocation length. As the initial length given before relaxation is smaller, the higher stress is needed to dissociate the junction.

References

[1] V. V. Bulatov, L. L. Hsiung, M. Tang, A. Arsenlis, M. C. Bartelt, W. Cai, J. N. Florando, M. Hiratani, M. Rhee, G. hommes, T. G. Pierce, and T. D. Rubia, *Dislocation multi-junctions and strain hardening*, Nature **440** (2006), 1174–1178.

[2] W. Cai and V. V. Bulatov, *Mobility laws in dislocation dynamics simulations*, Mater. Sci. Eng. **A 387-389** (2004), 277–281.

[3] J. R. Greer, *Size dependence of strength of gold at the micron scale in the absence of strain gradients*, Ph.D. thesis, Stanford University, Department of Materials Science and Engineering, 2005.

[4] M. D. Uchic, D. M. Dimiduk, J. N. Florando, and W. D. Nix, *Sample dimensions influence strength and crystal plasticity*, Science **13** (2004), 986–989.

5 Appendix (MATLAB codes)

5.1 The initial configuration of two dislocations

```
% Make dislocations
t = [-1:0.1:1]*pi;

x = 2000*(-cos(t)/sqrt(2)-sin(t)/sqrt(6));
y = 2000*(cos(t)/sqrt(2)-sin(t)/sqrt(6));
z = 2000*(2*sin(t)/sqrt(6));

x1 = 2000*(-cos(t)/sqrt(2)+sin(t)/sqrt(6));
y1 = 2000*(cos(t)/sqrt(2)+sin(t)/sqrt(6));
z1 = 2000*(2*sin(t)/sqrt(6));

figure(2)
plot3(x,y,z,'-o', x1,y1,z1,'-o');
xlim([-2500 2500]);ylim([-2500 2500]);zlim([-2500 2500]);
grid on
view([30 -30 40]) ;

D1 = [x' y' z'];
D2 = [x1' y1' z1'];

% Get phi
phi1 = t';
phi2 = t';

phi11 = phi1*ones(1,21);
phi22 = ones(21,1)*phi2';

% initialize junction length
junc_length = phi11*phi22;
```

5.2 The initial configuration dependence on the junction lengths

```
totalsteps=100;

appliedstress = zeros(3,3);

mobility='mobfcc1';

make_dis;
```

```
for dis1_no=1:21;
    for dis2_no=1:21;

rn = [  D1(dis1_no,:)                  7
        0      0      0     0
       -D1(dis1_no,:)                  7
        D2(dis2_no,:)                  7
        0      0      0     0
       -D2(dis2_no,:)                  7 ];

b1 = [  1   0  -1  ]/2;
b2 = [  0   1   1  ]/2;

n1 = [  1   1   1  ];  % no glide constraint
n2 = [  1   1  -1  ];  % no glide constraint

links = [ 1 2   b1 n1
          2 3   b1 n1
          4 5   b2 n2
          5 6   b2 n2 ];

maxconnections=8;
lmax = 1000;
lmin = 200;
a=lmin/sqrt(6);
MU = 27*10^9; % for gold
NU = 0.44; % for gold
Ec = MU/(4*pi)*log(a/0.1);

areamin=lmin*lmin*sin(60/180*pi)*0.5; % minimum discretization area
areamax=20*areamin; % maximum discretization area
dt0=1e-5;           %maximum time step
rmax=10.0;         %maximum allowed displacement per timestep
plotfreq=1;       %plot nodes every how many steps
plim=2500;          %plot x,y,z limit (nodes outside not plotted)

viewangle=[-40 30];
printfreq=1;      %print out information every how many steps
printnode=3;

integrator='int_trapezoid';

rann = 10;       %annihilation distance (capture radius)
%rntol=1e-1;       %tolerance for integrating equation of motion
```

```
rntol = 2*rann;      % on Tom's suggestion
rmax=30;

doremesh    =1;
docollision =1;
doseparation=1;

% run DDLAB simulation
dd3d;

move_pos = find(rn(:,4)==0);
move_coord = [rn(move_pos,1) rn(move_pos,2), rn(move_pos,3)];
junc_pos = find(-10^-2<move_coord(:,3) & move_coord(:,3)<10^-2 );

    if length(junc_pos)==1;
        junc_length(dis1_no,dis2_no)=0;

    elseif isempty(junc_pos)==0;
        junc_coord = [move_coord(junc_pos,1) move_coord(junc_pos,2),...
         move_coord(junc_pos,3)];
        junc_max = find(max(junc_coord(:,1)));
        junc_length(dis1_no,dis2_no) = sqrt(2)*...
        sqrt(junc_coord(junc_max,1)^2+junc_coord(junc_max,3)^2...
        +junc_coord(junc_max,3)^2);

    elseif isempty(junc_pos)==1;
        junc_length(dis1_no,dis2_no)=0;

    end

    end
end


% Modification of junction lengths at the extreme angles
junc_length(1,1)=2000;
junc_length(21,1)=2000;
junc_length(1,21)=2000;
junc_length(21,21)=2000;
junc_length(11,11)=2000;


% Plot the initial configuration-dependent junction length
figure(2)
surf(phi11,phi22,junc_length/2000);
```

```
colormap jet;
axis([-pi pi -pi pi 0 1]);
xlabel('\phi_{1}');ylabel('\phi_{2}');zlabel('l_{j}/l_{0}');
grid on;
view([5 30 40]);
```